

Importance of Model Fidelity of Power to X Devices in Energy System Analysis

Gusain, Digvijay; Cvetkovic, Milos; Yağci, Bekir Caner; Palensky, Peter

DOI

[10.1109/ISGT50606.2022.9817485](https://doi.org/10.1109/ISGT50606.2022.9817485)

Publication date

2022

Document Version

Final published version

Published in

2022 IEEE Power and Energy Society Innovative Smart Grid Technologies Conference, ISGT 2022

Citation (APA)

Gusain, D., Cvetkovic, M., Yağci, B. C., & Palensky, P. (2022). Importance of Model Fidelity of Power to X Devices in Energy System Analysis. In *2022 IEEE Power and Energy Society Innovative Smart Grid Technologies Conference, ISGT 2022* Article 9817485 (2022 IEEE Power and Energy Society Innovative Smart Grid Technologies Conference, ISGT 2022). IEEE. <https://doi.org/10.1109/ISGT50606.2022.9817485>

Important note

To cite this publication, please use the final published version (if applicable).
Please check the document version above.

Copyright

Other than for strictly personal use, it is not permitted to download, forward or distribute the text or part of it, without the consent of the author(s) and/or copyright holder(s), unless the work is under an open content license such as Creative Commons.

Takedown policy

Please contact us and provide details if you believe this document breaches copyrights.
We will remove access to the work immediately and investigate your claim.

Green Open Access added to TU Delft Institutional Repository

'You share, we take care!' - Taverne project

<https://www.openaccess.nl/en/you-share-we-take-care>

Otherwise as indicated in the copyright section: the publisher is the copyright holder of this work and the author uses the Dutch legislation to make this work public.

Importance of Model Fidelity of Power to X Devices in Energy System Analysis

Digvijay Gusain, Miloš Cvetković, Bekir Caner Yağci, Peter Palensky
Intelligent Electrical Power Grids, Electrical Sustainable Energy, TU Delft
Delft, The Netherlands
{D.Gusain, M.Cvetkovic, P.Palensky}@tudelft.nl, caneryagci1@gmail.com

Abstract—Power-to-X (PtX) technologies are accelerating the energy transition. Increasingly, these technologies are also being leveraged as flexible energy resources to support the electrical grid. PtX models are often represented using a constant efficiency term as a linear relation between the power input and energy output. However, the operational performance of any PtX device such as an electrolyser or an electric heat pump can depend on factors such as operational temperature. In this paper, we have developed and analyzed two levels of model fidelity of the most widely assessed PtX technologies: electrolyser and heat pump systems. We assess the impact of detailed models on operation of PtX within simulation-based energy system analysis. Our results show that for electrolyser systems, the efficiency errors can be almost 0.6%. With heat pump systems, the difference in COP can be as high as 1.4.

Index Terms—electrolyser, heat pump, model fidelity, power to x, temperature dynamics

I. INTRODUCTION

Power-to-X (PtX) are sector coupling technologies enabling the electrification of the energy system. These consist of electricity conversion and energy storage technologies such as electrolysers, heat pumps, electric vehicles, batteries, compressed gas tanks, etc. These technologies allow coupling of electricity to other energy domains such as gas, heat, chemicals, etc. As the share of electricity from renewable energy sources (RES), especially from sun and wind, increases, the demand for flexibility in the power system will also increase [1]. PtX technology is seen as a viable source to supply this increasing demand for power system flexibility [2], [3].

By integrating PtX into the electrical power systems, over and under-generation from RES can be absorbed by the PtX devices by modulating their power consumption. Using storage systems as buffers, such a flexible operation of PtX can provide ample opportunities for effective demand side management [4], [5]. To properly assess the value of these technologies as sources of flexibility for the electric power systems, a detailed technical assessment is needed.

An issue with existing studies in this domain is that currently available models and methods in the literature [4], [6], [7], make significant simplifications on physical characteristics of these devices, particularly in the consideration of impacts of operational temperature and pressure conditions on device performance. These studies use simplified representations, such as equations with constant relation between the power input and energy output. Some use generic models that highly

depend on manufacturer's data [8]–[10], where performance is measured in ideal conditions, and often performance metrics are averaged over testing periods of a year (such as with heat pump coefficient of performances). In reality, performance of a PtX highly depends on operational conditions such as ambient temperature, pressure conditions within the device, etc. Simplifications like these, which are made during modelling in any simulation-based technical or techno-economic analysis, can lead to a loss of some essential information. This results in higher operational costs, miscalculation of capacity [11] etc. which can further lead to inaccurate outcomes from these assessments. When PtX devices are even more pervasive than now, the impact of these erroneous assessments will be higher. Therefore, there is a need for accurate modeling of these technologies in any energy system analysis.

The main contributions of this paper is to develop and compare different models of PtX devices to determine the extent to which model fidelity impacts energy system analysis. We particularly look into investigating the effect of temperature simplifications in PtX models.

II. MODELING

In this section, we will develop and compare the models of two most widely assessed power to X technologies: the power to gas electrolyser and the power to heat electric heat pumps.

A. Electrolyser System

A large scale 50 MW proton-exchange membrane (PEM) electrolyser is modelled. In order to model this electrolyser, it is assumed that electrolyser cells are assembled into stacks and connected in series and parallel configuration for 50 MW capacity. We also assume that a scaled electrolyser system consisting of stacks of electrolyser cells behaves exactly similar to a single electrolyser stack.

We consider and model 4 physical domains of the electrolyser: electrochemical, pressure, massflow and thermal. Each sub-model has input and output variables that connected to one another within OpenModelica as illustrated in Fig. 1.

We further categorize models into two: Model A and Model B. Model A represents the simplistic model, while Model B represents the detailed model of the electrolyser system.

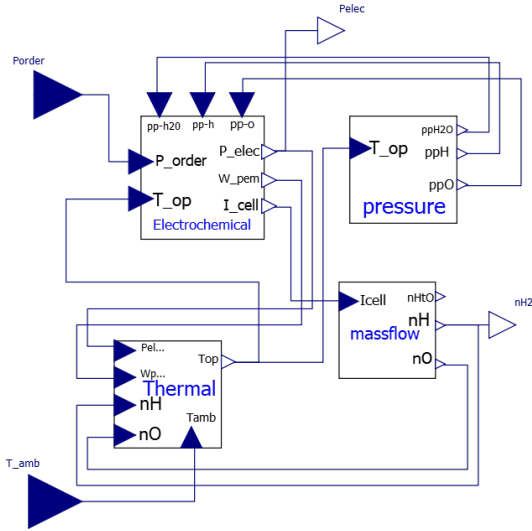


Fig. 1: Electrolyzer model developed in OpenModelica. For Model A, T_{amb} is constant, for Model B, T_{amb} is variable.

1) *Electrochemical Model*: The electrolyser cell voltage is given by Eq. (1).

$$V_{cell}(T) = V_{ocv}(T, p) + V_{act}(T) + V_{ohm}(T) \quad [V] \quad (1)$$

Here, open-circuit voltage V_{ocv} is the voltage necessary to start the water electrolysis reaction under ideal conditions. It is calculated using Nernst equation. The energy losses within the PEM stack can be modelled using overpotentials. Activation overpotential, V_{act} , is the energy necessary to start the electrochemical reaction and is given in Eq. (2). It is the dominant overpotential at low current densities.

$$V_{act} = \frac{R \cdot T_{op}}{2 \cdot \alpha_{an} \cdot F} \cdot \operatorname{asinh} \left(\frac{i_{dens}}{2 \cdot i_{0,an}} \right) \quad [V] \quad (2)$$

Here, i_{dens} is the current density of stack electrodes expressed in A/m^2 , $i_{0,an}$ is the exchange current density, and α_{an} is the charge transfer coefficient of the anode.

The ohmic overpotential, V_{ohm} , is the energy loss due to resistance of the cell membrane, and it is dominating at nominal current densities. Ohmic overpotential is calculated using Ohm's Law, as shown in Eq. (3).

$$V_{ohm} = R_{mem} \cdot i_d \quad [V] \quad (3)$$

Here, R_{mem} is the membrane resistance, calculated from membrane conductivity σ_{mem} and the membrane thickness δ_{mem} . In this paper, we have used the parameters for Nafion 117 membrane ($\delta_{mem} = 178 \cdot 10^{-6}m$). The temperature dependence of membrane conductivity can be modelled using Arrhenius expression [12].

Finally, the concentration (diffusion) overpotential occurs when electrolysis reaction is fast and the mass transport is relatively slow. Its effect is dominant at high current densities. Concentration overpotential is ignored in this study, assuming

nominal cell current never reaches high current densities that concentration overpotential is dominant.

The electrolyser cell current and active power consumption is calculated using Eqs. (4) and (5).

$$I_{cell} = A_{mem} \cdot i_{dens} \quad [A] \quad (4)$$

$$P_{cell} = I_{cell} \cdot V_{cell} \quad [W] \quad (5)$$

Here, A_{mem} in Eq. (4) is the membrane area (taken as 290 cm^2 in this paper).

2) *Pressure Model*: The input of pressure submodel is stack operation temperature T_{op} and the output is the partial pressures of water, hydrogen and oxygen as described in Eqs. (6) to (8).

$$pp_{H_2O} = 6.1078 \cdot 10^{-3} \cdot \exp \left(17.2694 \cdot \frac{T_{op} - 273.15}{T_{op} - 34.85} \right) \quad [bar] \quad (6)$$

$$pp_{H_2} = P_{cat} - pp_{H_2O} \quad [bar] \quad (7)$$

$$pp_{O_2} = P_{an} - pp_{H_2O} \quad [bar] \quad (8)$$

3) *Massflow Model*: The massflow submodel describes the mass transfer phenomena occurring in electrolysis cell with Eqs. (9) and (11). The input of this submodel is cell current calculated in electrochemical submodel. η_f is the Faraday efficiency and is assumed to be 1. n_{cells} is the number of electrolyser cells.

$$\dot{n}_{H_2} = \frac{n_{cells} \cdot I}{2 \cdot F} \cdot \eta_f \quad [mol/s] \quad (9)$$

$$\dot{n}_{O_2} = \frac{n_{cells} \cdot I}{4 \cdot F} \cdot \eta_f \quad [mol/s] \quad (10)$$

$$\dot{n}_{H_2O} = \frac{n_{cells} \cdot I}{2 \cdot F} \cdot \eta_f \quad [mol/s] \quad (11)$$

4) *Thermal Model*: The electrochemical, pressure and massflow submodels are the same for both Model A and Model B. However, for Model B, the thermal domain is also created with a lumped thermal capacitance model. Temperature of the electrolyser system is modelled with Eq. (12). The first term on the right side, $Q_{el,h}$, describes the heat generated by electrolysis reaction, and it depends on cell voltage and current. The second term, $W_{p,l}$, stands for the work contribution of the circulation pump. The third term, Q_c , represents for the heat removed by cooling system, and it has linear relation with the consumed active power. The fourth term, Q_l , is for the heat lost to ambient, and it depends on operational temperature T_{op} and ambient temperature T_{amb} . The last term comes from enthalpy lost with the products leaving the system, it has an empirical equation that depends on the operating temperature. For more details, reader is referred to [13]. Considering Eqs. (1) and (11) and adding the thermal dynamic submodel defined

in Eq. (12), turns the electrolyser system into a non-linear dynamic model, since each submodel depends on temperature parameter directly or indirectly.

$$C_{th} \frac{dT}{dt} = Q_{el,h}(V, I) + W_{p,l} - Q_c(P) - Q_l(T) - \sum_j \dot{n}_j \cdot \Delta h_j \quad (12)$$

B. Electric Heat Pumps

The coefficient of performance (COP) of an electric heat pump depends on the choice of refrigerant and the Rankine cycle efficiency (Carnot efficiency) of the refrigerant inside the heat pump, as described in Eq. (13).

$$COP = \frac{Q_{prod}}{W_p} \quad (13)$$

Here, Q_{prod} is the heat output and W_p is the electrical power consumed by the pump. In this paper, the refrigerant used for modeling is R134a, a common refrigerant in heat pumps. Two different models are developed. For the simplified model, a constant COP and no change in temperature is assumed. This model is called Model A and described with Eq. (14).

$$P = \frac{Q_{prod}}{COP_{avg}} \quad (14)$$

In reality, the COP strongly depends on the temperature of the energy source. Using the pressure-enthalpy table of R134a, COP values are calculated for various T_{amb} conditions. This data is then used to create a fifth order polynomial function of COP that depends on ambient temperature, as shown in Eq. (15).

$$COP^{real}(T_{amb}) = a_1 T_{amb}^5 + a_2 T_{amb}^4 + a_3 T_{amb}^3 + a_4 T_{amb}^2 + a_5 T_{amb} + a_6 \quad (15)$$

This is called Model B and is represented by Eq. (16).

$$P = \frac{Q_{prod}}{COP^{real}(T_{amb})} \quad (16)$$

Using MATLAB's curve fitting function, the coefficients $a_1, a_2, a_3, a_4, a_5, a_6$ of Eq. (15) are calculated to 3.46e-8, 1.29E-6, 4.35E-5, 2.387E-3, 1.186E-1, and 5.063 respectively.

III. EXPERIMENT SETUP

Each of Model A and Model B for both the electrolyser system and the electric heat pump system is given the same load profile. From this given load profile, we can measure the output gas (or heat) generated by the electrolyser (or heat pump), and compare the results.

A. Demand Profiles

The gas demand for the electrolyser is assumed to come from an industrial process, whereas the heat demand for PtH heat pump comes from district heating. This allows us to make reasonable assumptions to generate demand profiles.

To generate artificial demand profiles for each of the power to x models, the approach adopted in reference [14] is used in this work. The benefit of this approach is that it only requires historical ambient temperature data to generate the time-series scheduled energy demand profiles. Equation (17) describes the model in reference [14]. Here, Q_{dem} is the heat demand, but can also be replaced by $H2_{dem}$ to obtain gas demand.

$$Q_{dem} = Q_b + \frac{Q_{max} - Q_{base}}{T_{ref} - T_{min}} \cdot \max(0, T_{ref} - T(t)) \quad (17)$$

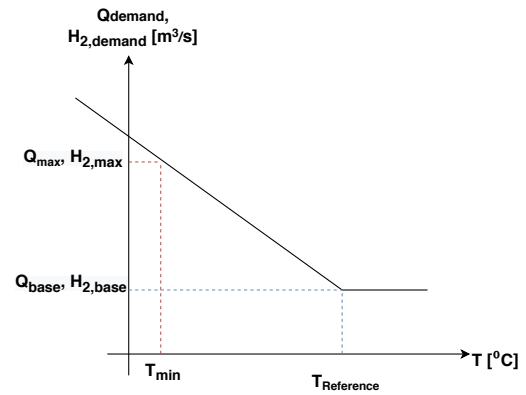


Fig. 2: The relation between ambient temperature and hydrogen and heat demand [15]

We provide the power set points and temperature values to the models for 7 days. For the electrolyser system, Model A is given a constant temperature input, while Model B is given a variable temperature input Fig. 3. For the heat pump system, Model A is given a daily average temperature input, while Model B is given an hourly temperature time series.

The simulations are performed on a Windows 10 PC with Intel Xeon CPU E5-1620 vs 3.50GHz.

IV. RESULTS AND DISCUSSION

The effect of operational temperature evolution on efficiency curve of electrolyser and ambient temperature evolution on COP of heat pump can be observed in figures 4 and 6 respectively.

The efficiency plots of the two models are shown in Fig. 4. We observe that due to the temperature deviation, the maximum efficiency difference between the performance of two models is 0.6%. Although, this may not seem a significant difference, this difference will be substantial if electrolyser capacities of hundreds of MWs are employed in large numbers. The analysis is also impacted by the design and size of the auxiliary units for temperature regulation within the electrolyser system. Consider the cooling system.

TABLE I: Ambient temperature - demand relation parameters

	T_{ref} [$^{\circ}C$]	T_{min} [$^{\circ}C$]	Base Demand [m^3/s]	Max Demand [m^3/s]
Industrial PtG	25	5	3.13E-03	3.85E-03
District Heating PtH	25	5	3	4

If the cooling capacity of the designed system is calculated to be less than required, it would lead to larger temperature differences between Model A and Model B, resulting in bigger variations in efficiency curves.

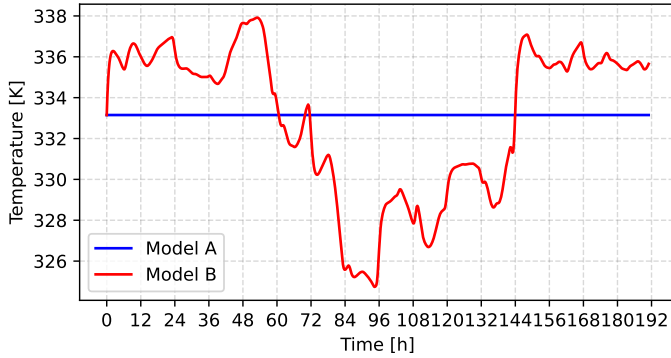


Fig. 3: Temperature inputs for electrolyser Model A and Model B

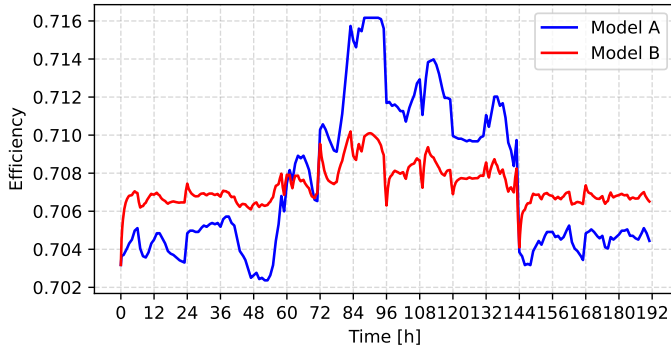


Fig. 4: Efficiency comparison of electrolyser models

Figure 5 reveals the difference between the active power consumption of Model A and Model B of the electrolyser. The maximum power consumption difference between them is 0.4 MW for a 50 MW electrolyser system. This corresponds to 0.8% of the total capacity. Although, again, not significant in this case, as the electrolyser capacity increases, this percentage would lead to a larger active power difference between models A and B.

Figure 6 compares the COP of Model A and Model B. In Model A, the COP is calculated from daily average temperature; therefore, it is constant during a day. In Model B, the hourly measured temperature is provided to calculate the COP. The maximum difference in COP values between Model A and Model B is 1.4. These results also show that temperature considerations have significant effect on COP characterization of heat pump.

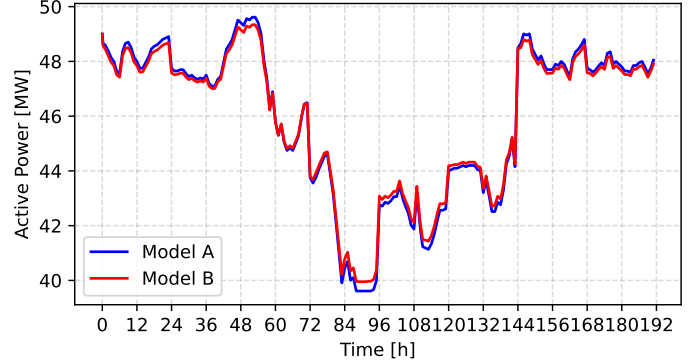


Fig. 5: Active power consumption characteristics of electrolyser system based on efficiency characteristics

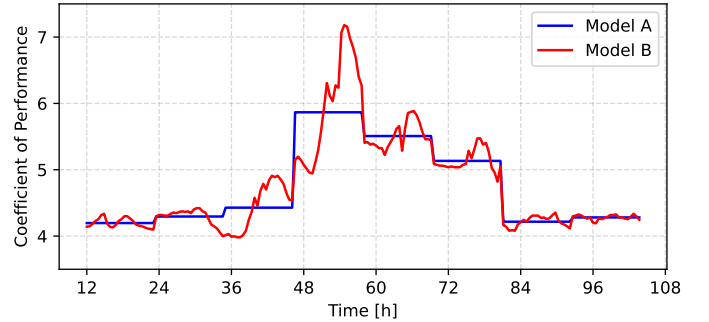


Fig. 6: COP values for Model A and Model B for heat pump systems

Figure 7 compares the active power consumption of PtH models. Maximum power consumption difference between model A and B is 9 MW. This is equal to a maximum error of 18% for a 50 MW electric heat pump system. These are significant numbers. Therefore, COP of a heat pump can be assumed constant if inlet and outlet temperatures remain stable during operation. Otherwise, COP must be calculated with respect to temperature levels of the energy source.

Figure 8 shows the demand curves of model B of each PtX technology. This figure validates that industrial hydrogen demand has fewer variations with respect to changing ambient temperature than district heating demand as expected from Section III-A.

The investigation of two different model resolutions has revealed that correct efficiency and COP characterization of PtX highly depends on operating temperature or pressure conditions. Therefore, these must be taken into consideration when conducting any simulation based analysis involving these technologies. We have shown that a constant operational temperature assumption caused 0.6% difference on efficiency results of electrolyser and ≈ 1.4 difference on coefficient of

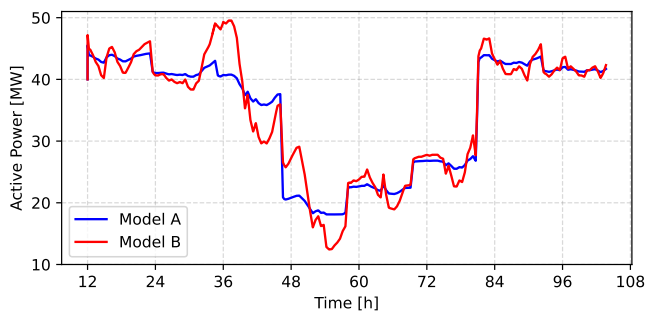


Fig. 7: Active power consumption characteristics of heat pump system based on COP characteristics

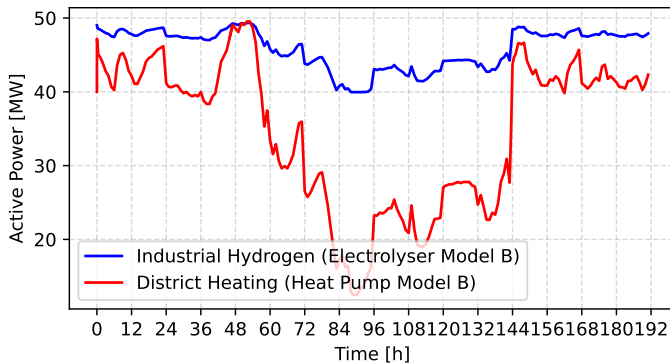


Fig. 8: Active power consumption for Model B of PtG and PtH

performance values of heat pump models. Depending on the size of installations, the impact of incorrect assessment can be low or very significant. Another interesting result has found on the hydrogen and heat production differences of the models for PtG and PtH. The maximum hydrogen and heat production difference was $0.032 \text{ m}^3/\text{s}$ and $0.20 - 0.96 \text{ m}^3/\text{s}$ for PtG and PtH models respectively. This means that there is a possibility of incorrectly sizing the integrated storage capacity for these PtX technologies, which can directly impact the economic viability studies of these systems.

V. CONCLUSIONS

In this paper, we set out to investigate the impact that modelling detail can have on analysis for power to x devices. Specifically, we explored the impact of thermal dynamics on these models. We achieved this by creating detailed models of PtX devices in OpenModelica and providing a synthetic demand profile and different ambient temperature inputs to measure their responses. We showed that using detailed models of these devices lead to better insights into how these systems will operate. In case of electrolyzers, we showed that the difference in efficiency characteristics between simple and detailed models can be as much as 0.6%. In case of electric heat pump models, we showed that COP can differ by as much as 1.4. These factors influence the amount of products produced by these technologies. Deviations in results from simple and detailed models can also impact economic viability

studies and integrated storage sizing problems. Therefore, it is important to use detailed models in energy system analysis of future energy systems.

ACKNOWLEDGMENT

The authors would like to thank NWO for providing the funding for this project.

REFERENCES

- [1] Alliander; ECN, "Demand and supply of flexibility in the power system of the Netherlands, 2015-2050," *Summary report of the FLEXNET project*, no. November 2017, p. 70, 2017.
- [2] P. D. Lund, J. Lindgren, J. Mikkola, and J. Salpakari, "Review of energy system flexibility measures to enable high levels of variable renewable electricity," *Renewable and Sustainable Energy Reviews*, vol. 45, pp. 785–807, 2015. [Online]. Available: <http://dx.doi.org/10.1016/j.rser.2015.01.057>
- [3] S. Byfield and D. Vetter, "Flexibility concepts for the german power supply in 2050: Ensuring stability in the age of renewable energies," *Deutsche Akademie der Technikwissenschaften: Munich, Germany*, 2016.
- [4] J. Salpakari, J. Mikkola, and P. D. Lund, "Improved flexibility with large-scale variable renewable power in cities through optimal demand side management and power-to-heat conversion," *Energy Conversion and Management*, vol. 126, pp. 649–661, 2016. [Online]. Available: <http://dx.doi.org/10.1016/j.enconman.2016.08.041>
- [5] G. Papaefthymiou, B. Hasche, and C. Nabe, "Potential of heat pumps for demand side management and wind power integration in the German electricity market," *IEEE Transactions on Sustainable Energy*, vol. 3, no. 4, pp. 636–642, 2012.
- [6] H. Kim, M. Park, and K. S. Lee, "One-dimensional dynamic modeling of a high-pressure water electrolysis system for hydrogen production," *International Journal of Hydrogen Energy*, vol. 38, no. 6, pp. 2596–2609, 2013. [Online]. Available: <http://dx.doi.org/10.1016/j.ijhydene.2012.12.006>
- [7] K. Onda, T. Murakami, T. Hikosaka, M. Kobayashi, R. Notu, and K. Ito, "Performance Analysis of Polymer-Electrolyte Water Electrolysis Cell at a Small-Unit Test Cell and Performance Prediction of Large Stacked Cell," *Journal of The Electrochemical Society*, vol. 149, no. 8, p. A1069, 2002.
- [8] B. W. Tuinema, E. Adabi, P. K. Ayivor, V. G. Suárez, L. Liu, A. Perilla, Z. Ahmad, J. L. R. Torres, M. A. Van Der Meijden, and P. Palensky, "Modelling of large-sized electrolyzers for realtime simulation and study of the possibility of frequency support by electrolyzers," *IET Generation, Transmission and Distribution*, vol. 14, no. 10, pp. 1985–1992, 2020.
- [9] M. Chamoun, R. Rulliere, P. Haberschill, and J. F. Berail, "Dynamic model of an industrial heat pump using water as refrigerant," *International Journal of Refrigeration*, vol. 35, no. 4, pp. 1080–1091, 2012. [Online]. Available: dx.doi.org/10.1016/j.ijrefrig.2011.12.007
- [10] F. D. C. Lopes and E. H. Watanabe, "Experimental and theoretical development of a PEM electrolyzer model applied to energy storage systems," *2009 Brazilian Power Electronics Conference, COBEP2009*, no. 2, pp. 775–782, 2009.
- [11] P. Schott, J. Sedlmeir, N. Strobel, T. Weber, G. Fridgen, and E. Abele, "A generic data model for describing flexibility in power markets," *Energies*, vol. 12, no. 10, pp. 1–29, 2019.
- [12] R. García-Valverde, N. Espinosa, and A. Urbina, "Simple PEM water electrolyser model and experimental validation," *International Journal of Hydrogen Energy*, vol. 37, no. 2, pp. 1927–1938, 2012.
- [13] J. Webster and C. Bode, "Implementation of a Non-Discretized Multiphysics PEM Electrolyzer Model in Modelica," *Proceedings of the 13th International Modelica Conference, Regensburg, Germany, March 4–6, 2019*, vol. 157, pp. 833–840, 2019.
- [14] B. Felten, J. P. Baginski, and C. Weber, "KWK-Mindest- und Maximal einspeisung - Die Erzeugung von Zeitreihen für die Energiesystemmodellierung," no. 10, 2017.
- [15] J. Weibezahn, "Data Documentation 92: Electricity, Heat, and Gas Sector Data for Modeling the German System," *DIW Berlin*, 2017, no. ISSN 1861-1532, 2017.